Retrieval of solar-induced chlorophyll fluorescence from TanSat space measurement

Lu Yao (yaolu@mail.iap.ac.cn), Yi Liu, Dongxu Yang

LAGEO, Institute of Atmospheric Physics, Chinese Academy of Science, Beijing, China

Introduction

Solar-induced chlorophyll fluorescence (SIF), re-emitted during the conversion of sunlight to chemical energy in plant leaves, constitutes a very small additional offset to the reflected radiance, which can be observed by sensitive remote sensing detectors.

A hyper-spectrum grating spectrometer (ACGS) onboard the Chinese global carbon dioxide monitoring satellite (TanSat) provides high spectrum resolution ~0.038nm and signal-to-noise ratio (SNR) ~360 in O2-A band and it makes it possible to getting SIF from space measurement with the best spatial resolution of 2 × 2 km.

Based on the IAP Carbon dioxide retrieval Algorithm for Satellite observation platform, an SIF retrieval algorithm (ATG-SIF) is developed for satellite measurement.

Objectives

This study aims to retrieval SIF from TanSat space measurement as well as OCO-2 with the same algorithm. The inter-comparison of SIF between two satellite missions and OCO-2 official product is carried out to test the reliability of satellite data and the algorithm. The global SIF distribution and its seasonal variation is also displayed and discussed here for subsequent regional analysis.

Methods

- **Principle and Forward model**

(1) The nadir measured radiance from space over the Lambertian surface

$$L_{TOA}^{\lambda} = I_0^{\lambda}\mu_0(\rho_0^{\lambda} + \frac{\rho_s^{\lambda}T_{\downarrow}^{\lambda}T_{\uparrow}^{\lambda}}{\pi}) + SIF_{TOA}^{\lambda}$$

(2) In the absence of inelastic atmospheric scattering, the ratio spectra of the Fraunhofer lines to the continuum level radiance could be fitted with a simple low-order polynomial in spectral space

$$L_{TOA}^{\lambda} = < I_0^{\lambda} > \cdot \sum_{i=0}^{n} a_i\lambda^i + SIF_{TOA}^{\lambda}$$

(3) Express the above formula in logarithmic form

$$\vec{f}(F_s^{rel}, a) = log\left(< \vec{I_0} + F_s^{rel} >\right) + \sum_{i=0}^{n} a_i\lambda^i$$

(4) SIF calculation

$$SIF = F_s^{rel} \cdot I_{cont}$$

- **The state vector**

State vector element	note
Relative SIF	Relative contribution of SIF to continuum
OD scale	Scale of O2 absorption
polynomial coefficient	Coefficient of the low-order polynomial
Wavenumber shift	Wavenumber shift caused by instrument movement

- **Wavelength Coverage**

KI Fraunhofer line (12982~12988 cm-1)

Reference

Frankenberg, C., Butz, A., Toon, G.C., 2011a. Disentangling chlorophyll fluorescence from atmospheric scattering effects in O 2 A-band spectra of reflected sun-light. Geophys. Res. Lett. 38http://dx.doi.org/10.1029/2010GL045896.

Results

- **Inter-comparison of SIF between OCO-2 and TanSat**

With the similar overpass time of OCO-2 and TanSat, it becomes convenient to make cross-mission comparison. Fig. 1 show that the SIF retrieved from TanSat and OCO-2 by the same algorithm have the similar patterns in spatial with the season. Furthermore, the SIF retrievals from two satellite missions own the same level of magnitude. Comparing to the relative low intensity of SIF signal without any validation, the SIF distribution pattern seems to be more significant. However, there are still some mismatch regions existing, especially over the Greenland in Northern hemisphere in spring and summer. Because of the snow covered surface of Greenland, the SIF retrievals should be zero and used to the instrument bias calculation. While the bias correction is performed in the post processing, a portion of the systematic error from the ambiguous instrument condition still remains and has impact on the final SIF results.

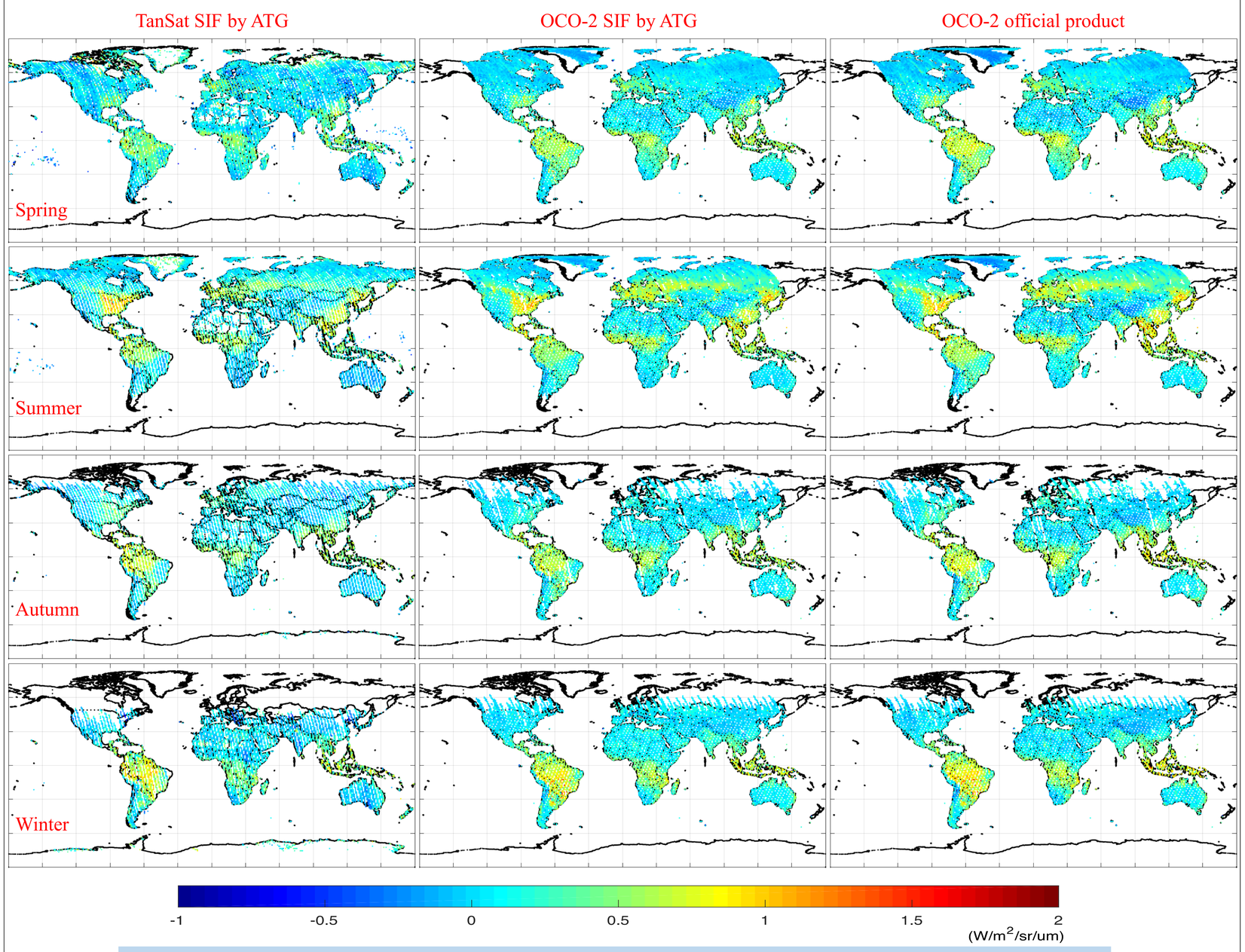

Fig. 1. The global seasonal SIF distribution of TanSat in the left column, OCO-2 in the middle column and OCO-2 official product in the right column with the spatial grid of 1 ° ×1 ° . Maps in each row shows SIF for spring, summer, fall and winter in northern hemisphere successively.

- **Global SIF distribution**

The global seasonal SIF maps from OCO-2 retrieval are shown on the middle panel in Fig.1, and the maps from OCO-2 public products are on the right panel in Fig.1. In generally, these maps of the same season agree well in spatial. Considering the growth state of vegetation along with the season and the global distribution of vegetation, the averaged seasonal SIF data is capable of presenting the overall SIF pattern and neglects the point-to-point relationship of SIF data.

- **Seasonal variation and regional analysis**

With one-year of SIF data from March 2017 to February 2018, the annual variation of SIF in spatial and temporal scale can be distinguished. As displayed in Fig.1, the spatial pattern of SIF varies with the time of year and the significant SIF emission area moves from north to south, due to the dominant influence of the vegetation growth status, while the regions of vegetation coverage near the equator maintain continuous SIF emission through the year. The seasonal averaged SIF in northern hemisphere increases from spring to summer and decreases in autumn and winter gradually. The highest SIF signal of northern hemisphere, about 0.8~1.8 Wm−2μm−1sr−1, is from the eastern US in summer where is covered by large area of croplands. In addition, there are also obvious SIF emission (0.5~1.2 Wm−2μm−1sr−1) observed in the central Europe, southern Asia and northeastern China during the summer. In these regions, the croplands and deciduous forests contributes to the SIF enhancement. In southern hemisphere, the strongest SIF emission occurs in Amazon for about 0.8~2 Wm−2μm−1sr−1 in winter, where is evergreen broad-leaf rainforest. The other region of distinct SIF emission is in Africa with the SIF value of 0.4~8 Wm−2μm−1sr−1 during the year, which is covered by evergreen broad-leaf rainforest and woody savannas. Further more, with the SIF distribution in Africa, the primary SIF emission area moves southward from summer to winter obviously. For the other regions like Sahara, polar zone and southwestern of China, where are covered by desert, snow or barren soil, the SIF value is approximately zero.

Conclusion

- **Based on the IAP Carbon dioxide retrieval Algorithm for Satellite observation platform, a SIF retrieval algorithm is developed for TanSat observation and can be applied to other satellite missions, such as OCO-2.**
- **The cross-mission comparison is carried out between OCO-2 and TanSat SIF retrievals to test the reliability of the TanSat data and the algorithm.**
- **One-year of SIF data is retrieved from TanSat and OCO-2 for global SIF distribution and its seasonal variation analysis. These analysis make it evident that data quality control and instrument bias correction is significant for SIF.**